Inhibitor discovery of phospholipases and N-acyltransferases
Zhou, J.

Citation
Zhou, J. (2020, November 11). *Inhibitor discovery of phospholipases and N-acyltransferases*. Retrieved from https://hdl.handle.net/1887/138014

Version:	Publisher's Version
License:	[Licence agreement concerning inclusion of doctoral thesis in the Institutional Repository of the University of Leiden](#)
Downloaded from:	https://hdl.handle.net/1887/138014

Note: To cite this publication please use the final published version (if applicable).

Cover Page

Universiteit Leiden

Author: Zhou, J.
Title: Inhibitor discovery of phospholipases and N-acyltransferases
Issue date: 2020-11-11

5

Development of a PLA2G4E assay and subsequent application in hit identification

5.1 Introduction

In 1996, Piomelli and coworkers characterized the Ca^{2+}-dependent biosynthesis of *N*-acylphosphatidylethanolamines (NAPE) in cortical neurons and rat brain tissue.[1, 2] The enzyme responsible for the Ca^{2+}-dependent formation of NAPEs remained elusive until Cravatt and colleagues showed that PLA2G4E (also known as cPLA₂ε) was able to transfer an acyl chain from the *sn*-1 position of phosphatidylcholine (PC) to the amine of phosphatidylethanolamine (PE), thereby effectively producing NAPEs.[3]

PLA2G4E was previously discovered in a comprehensive homology search against murine genome and EST databases and annotated as a phospholipase A (PLA).[4] It belongs to the cytosolic phospholipase A2 group IV (PLA2G4) proteins, a subfamily from the PLA2 proteins, which catalyze the hydrolysis of the *sn*-2 acyl bond of phospholipids, thereby releasing fatty acids. This leads to a cascade of lipid second messengers, which regulates a wide variety of physiological responses and plays an important role in diseases, such as cancer.[5] There are six members in this protein family, namely PLA2G4A, PLA2G4B, PLA2G4C, PLA2G4D, PLA2G4E and PLA2G4F. These proteins are structurally similar. They all contain a N-terminal C2 domain (except PLA2G4C) and a C-terminal catalytic domain. The C2 domain has a binding site for intracellular Ca^{2+}. When calcium ions bind, the protein is transported from the cytosol to the Golgi membrane, which is needed for catalytic activity.[6] The catalytic pocket contains a Ser/Asp dyad which lays in the α/β hydrolase fold.[6, 7] In contrast to the other family members, PLA2G4E has a strong preference for catalyzing the *N*-acyltransferase reactions over phospholipid hydrolysis.

PLA2G4E has high mRNA expression levels in heart, skeletal muscle, testis and thyroid and low expression in brain and stomach. PLA2G4E was previously found to play an important role within the clathrin-independent transport pathway, which is involved in the uptake and recycling of cargo proteins, such as MHC-I.[8] Two isoforms of human PLA2G4E (hPLA2G4E-A and hPLA2G4E-B) have been identified. Their activity is potently stimulated by phosphatidylserine (PS).[9] Endogenous PS and other anionic phospholipids (such as phosphatidic acid and phosphatidylinositol 4,5-bisphosphate) affect the localization and enzyme activity of PLA2G4E.[10] Currently, there are no inhibitors of PLA2G4E available that could help to elucidate the biological role of PLA2G4E. In this chapter, competitive activity based protein profiling (ABPP) is used to identify the first inhibitors of PLA2G4E.

5.2 Results and discussion

To test whether the fluorescently labeled fluorophosphonate probe TAMRA-FP could be used in a competitive ABPP experiment, TAMRA-FP was incubated with the membrane fraction of human embryonic kidney 293T (HEK293T) cells that transiently overexpressed human PLA2G4E fused to a FLAG-tag. Resolving the proteins by sodium dodecyl sulfate polyacrylamide gel

electrophoresis (SDS-PAGE) and in-gel fluorescent scanning revealed a fluorescent band at the expected MW, which overlapped with a band visualized by the FLAG-tag antibody. This band was absent in mock-transfected cells (Figure 2A, left). The labeling was dependent on both the probe and protein concentration (Figure 2A, right panels). A protein concentration of 0.25 µg/µL and probe concentration of 0.05 µM were chosen as the optimal ABPP conditions. Removal of Ca^{2+}-ions from the incubation buffer resulted in a strong decrease in labeling, thereby confirming the Ca^{2+}-dependency of the enzyme activity (Figure 2B). Fluorescent labeling of the protein was optimal at 3 mM Ca^{2+} and at pH 8.0 (Figure 2C-D). A 5 min incubation was sufficient to generate a robust fluorescent signal. Taken together, these results demonstrated that TAMRA-FP can efficiently label active human PLA2G4E and optimal ABPP assay conditions were found that could be used to identify inhibitors of PLA2G4E.
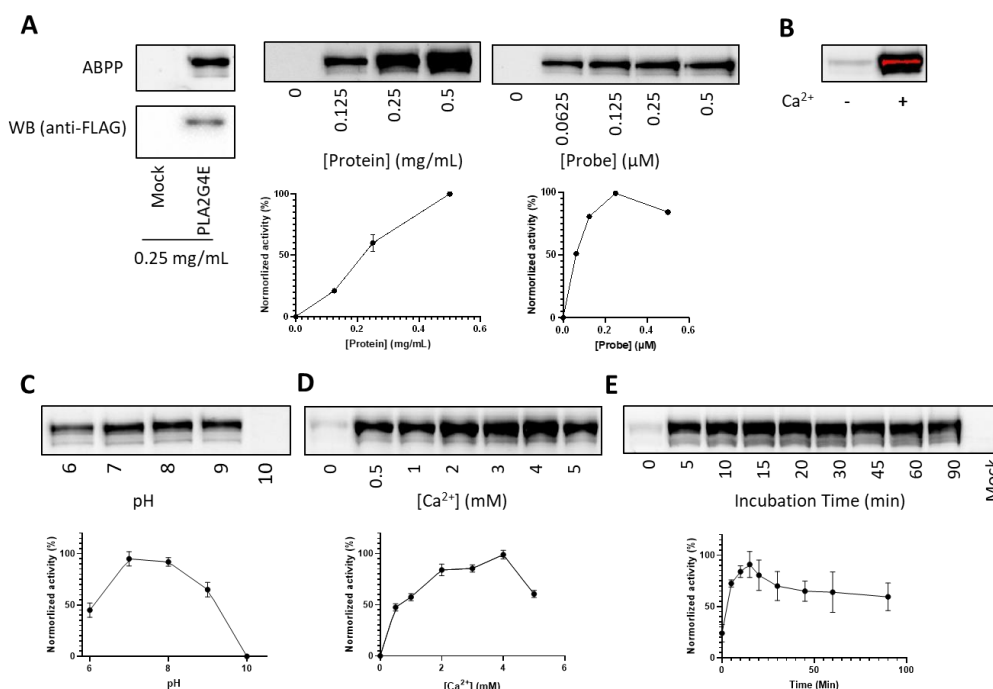

Figure 2. (A) Confirmation of hPLA2G4E overexpression with ABPP and western blot (left) and ABPP labeling of hPLA2G4E with probe TAMRA-FP at different probe or protein concentrations (right) (N=2). For protein concentration optimization 500 nM TAMRA-FP was used. For probe concentration optimization 0.25 mg/mL protein was used. (B) Gel-based ABPP to test the difference in labeling with TAMRA-FP (0.5 µM, 20 min at RT) on the membrane fraction of hPLA2G4E (1 µg/µL) overexpression lysate in the presence or absence of calcium ($CaCl_2$, 3 mM). (C, D, E) Optimization of ABPP conditions for hPLA2G4E using probe TAMRA-FP. For pH optimization 500 nM TAMRA-FP, 1 mg/mL protein and 3 mM $CaCl_2$ were used; for Ca^{2+} concentration optimization 500 nM TAMRA-FP and 0.5 mg/mL protein were used; for incubation time optimization 62.5 nM TAMRA-FP, 0.25 mg/mL protein and 3 mM $CaCl_2$ were used (N=2).

Next, a focused library of 223 compounds[11] was screened at 10 µM in a competitive gel-based ABPP format. Compounds that inhibited fluorescent labeling of PLA2G4E over 50% were retested. Eight compounds (**6**, **7**, **8, 45**, **177**, **180**, **195** and **196**) reduced protein activity by more than 80% and were designated as potential hits (Figure 3; Table 1). These compounds could be divided into two different clusters based on their scaffolds: compounds **45**, **177**, **180**, **195** and **196** belong to the triazoleurea class of inhibitors, whereas compounds **6**-**8** constitute the bromoenol lactone class.
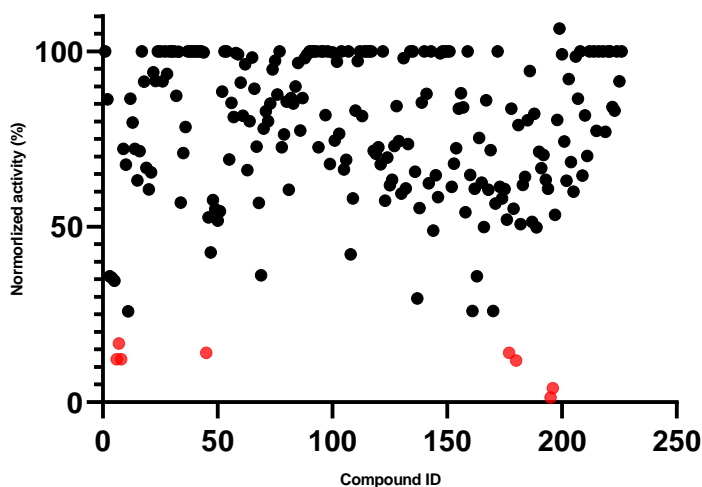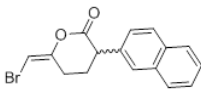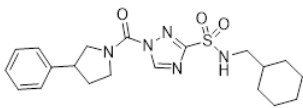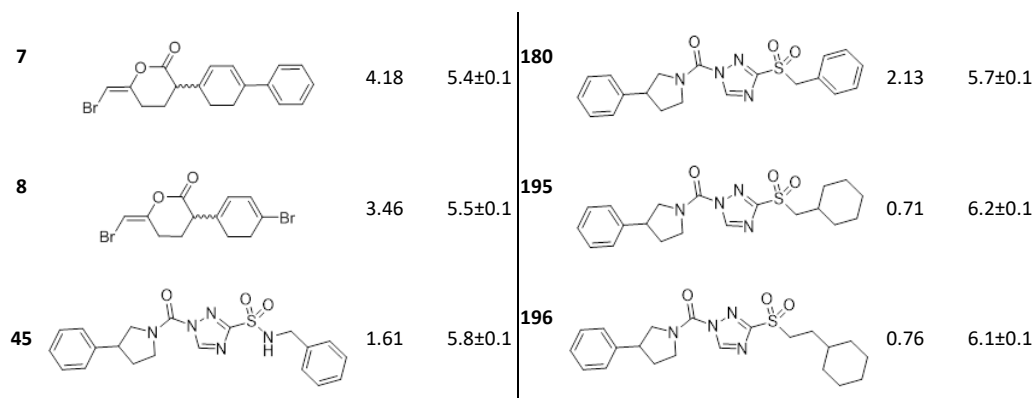

Figure 3. Summary of all tested compounds (10 µM) with corrected residual protein activity of hPLA2G4E (N=1). The data is presented in percentage (%) and lower percentage indicates higher inhibitory activity. The potential hits (>80% inhibition) are highlighted in red.

The compounds showing more than 80% inhibition at 10 µM were tested in a concentration-response manner to determine their IC_{50} values (Table 1). (The IC_{50} curves are shown in Figure S1).

Table 1. The chemical structures, IC_{50} values and pIC_{50} values with standard deviations of 8 inhibitors of hPLA2G4E (N=3).

ID	Structures	IC_{50} (µM)	pIC_{50}	ID	Structures	IC_{50} (µM)	pIC_{50}
6		5.04	5.3±0.1	**177**		1.56	5.8±0.1

7	(structure)	4.18	5.4±0.1	**180**	(structure)	2.13	5.7±0.1
8	(structure)	3.46	5.5±0.1	**195**	(structure)	0.71	6.2±0.1
45	(structure)	1.61	5.8±0.1	**196**	(structure)	0.76	6.1±0.1

Compound **195** and **196** were the most potent inhibitors with pIC$_{50}$ values of 6.2 ± 0.1 and 6.1 ± 0.1, respectively. In order to better profile the selectivity of these compounds, not only the most compounds (**195** and **196**) but also compounds from other scaffolds (**6-8** and **45)** were subjected to gel-based ABPP using mouse brain membrane and cytosol proteome (Figure 4).
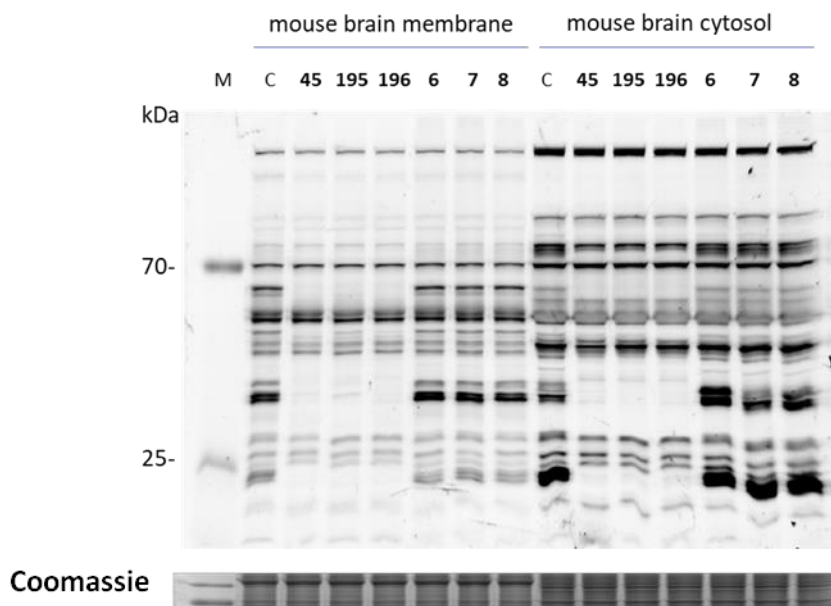

Figure 4. Selectivity of six inhibitors on mouse brain membrane and cytosol. The results of ABPP gel of the inhibitors (10 µM of **6**, **7**, **8**, **45**, **195** and **196**) on mouse brain proteins of the membrane and cytosol (2.5 µg/µL). This is detected by reactions with TAMRA-FP (0.5 µM, 20 min at RT). The samples have been loaded on a 10% SDS-PAGE gel. Coomassie staining was done as protein loading control.

At 10 µM, compounds **45**, **195** and **196** reduced fluorescence labeling of proteins with a MW around 25, 35, 60 and 75 kDa in the mouse brain membrane proteome. Compounds

6-8 showed no off-targets at 10 µM. Of note, compound **6** increases the labeling of a protein at around 35 kDa in the cytosol. Overall, the compounds **6-8** are more selective than compounds **45**, **195** and **196**.

To gain more insight into the selectivity of these compounds over the other proteins of the PLA2G4 family an ABPP method was developed as described above for mouse PLA2G4A-D and human PLA2G4A, C and D. In total, four proteins (mPLA2G4B, hPLA2G4C, mPLA2G4C and mPLA2G4D) could be successfully labeled (Figure 5) (See SI Figure S2 for optimization results).
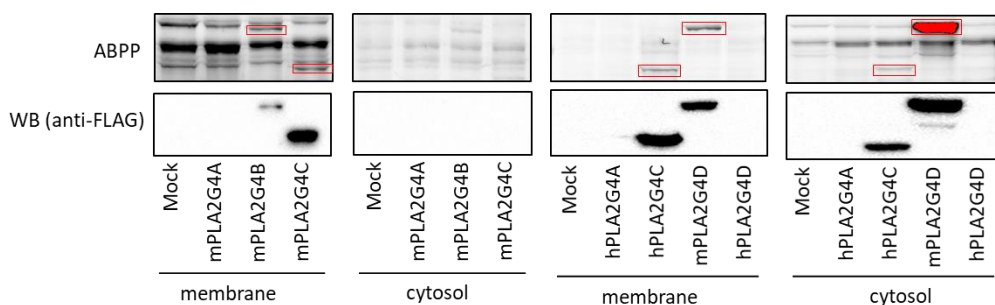

Figure 5. Gel-based ABPP for PLA2G4 protein family members. mPLA2G4B, mPLA2G4C, hPLA2G4C, and mPLA2G4D could be labelled with TAMRA-FP (0.5 µM, 20 min at RT). The samples were loaded on a 10% SDS-PAGE gel. The labeled PLA2G4 proteins are marked with a red box.

Neither of the eight compounds showed any activity on mPLA2G4B and mPLA2G4C (Table S1). Five compounds inhibited mPLA2G4D with more than 80% and were tested in a concentration-response manner (Table 2, inhibition curves in Figure S3). Compounds **6-8** showed submicromolar activity on mPLA2G4D (pIC$_{50}$: 6.1-6.3), whereas compounds **195** and **196** showed somewhat lower activity (pIC$_{50}$< 6).

Table 2. pIC$_{50}$ values for the compounds which showed inhibition for mPLA2G4D (N=3).

compound	6	7	8	195	196
pIC50 + S.D.	6.3 ± 0.1	6.3 ± 0.1	6.1 ± 0.1	5.8 ± 0.1	5.8 ± 0.1

5.3 Conclusions

This chapter reported on the discovery of the first inhibitors of PLA2G4E. A competitive, gel-based ABPP method for PLA2G4E using TAMRA-FP was successfully developed and applied to screen a focused library of lipase inhibitors. This resulted in the discovery of two clusters of inhibitors with different scaffolds. The triazoleurea inhibitors were the most potent inhibitors with submicromolar activity, whereas the bromoenol lactone inhibitors were less potent, but more selective as determined by gel-based ABPP using mouse brain proteomes. Optimization of the potency and selectivity of the inhibitors is required to be able to use them to study the biological role of PLA2G4E in an acute and dynamic setting with these novel tools.

5.4 Experimental procedures

Plasmids. Full-length human cDNA of PLA2G4A, C-E, and mouse cDNA of PLA2G4A-D were cloned into mammalian expression vector pcDNA3.1, containing genes for ampicillin and neomycin resistance. The inserts were cloned in frame with a C-terminal FLAG-tag and site-directed mutagenesis was used to remove restriction sites by silent point mutations. Plasmids were isolated from transformed XL-10 Z-competent cells (Maxi Prep kit: Qiagen) and sequenced at the Leiden Genome Technology Center. Sequences were analyzed and verified (CLC Main Workbench).

Cell culture

General. HEK293T cells were kept in culture at 37 °C under 7% CO_2 in DMEM containing phenol red, stable glutamine, 10% (v/v) New Born Calf Serum (Thermo Fisher), and penicillin and streptomycin (200 µg/mL each; Duchefa). Medium was refreshed every 2-3 days and cells were passaged twice a week at 80-90% confluence. Cell lines were purchased from ATCC and were regularly tested for mycoplasma contamination.

Transient transfection. Transient transfection was performed as previously described.[12] In brief, HEK293T cells were seeded in 15-cm petri dishes one day prior to transfection. Prior to transfection, culture medium was aspirated and a minimal amount of medium was added. A 3:1 (m/m) mixture of polyethyleneimine (PEI, 1 mg/mL) (60 µg/15-cm dish) and plasmid DNA (20 µg/dish) was prepared in serum free culture medium and incubated for 15 min at RT. Transfection was performed by dropwise addition of the PEI/DNA mixture to the cells. Transfection with the empty pcDNA3.1 vector was used to generate control samples (mock groups). After 24 h, medium was refreshed. Medium was aspirated 72 h post-transfection and cells were harvested by resuspension in PBS. Cells were pelleted by centrifugation (5 min, 1,000 × g) and the pellet was washed with PBS. Supernatant was discarded and cell pellets were snap-frozen in liquid nitrogen and stored at -80 °C until sample preparation.

Sample preparation

Cell membrane and cytosol proteome preparation. Cell pellets were thawed on ice, resuspended in cold lysis buffer (50 mM Tris HCl, pH 8, 2 mM DTT, 1 mM $MgCl_2$, 25 U/mL benzonase) and incubated on ice (30 min). The cell lysate was collected and centrifuged (100,000 × g, 45 min, 4 °C, Beckman Coulter, Ti 70.1 rotor). The supernatant was collected (cytosolic fraction) and the pellet (membrane fraction) was resuspended in cold storage buffer (50 mM Tris HCl, pH 8, 2 mM DTT) by thorough pipetting and passage through an insulin needle (29G). Protein concentrations were determined by a Quick Start™

Bradford Protein Assay or Qubit^{TM} protein assay (Invitrogen). Samples were flash frozen in liquid nitrogen and stored at -80 °C until further use.

Activity based protein profiling on transiently transfected HEK293T cell lysate. Gel-based activity based protein profiling (ABPP) was performed with minor alterations of the previously reported protocol.[12] For ABPP assays on HEK293T cells overexpressing the corresponding PLA2G4 proteins, the cytosol proteome (0.5 mg/mL, 20 μL) was pre-incubated with vehicle (DMSO) or inhibitor (0.5 μL in DMSO, 30 min, RT) followed by an incubation with the activity based probe TAMRA-FP for 5 min (PLA2G4E) or 20 min (PLA2G4A-D). Final concentrations for the inhibitors were indicated in the main text and figure legends. Reactions were quenched with 7 μL of 4x Laemmli buffer (5 μL, 240 mM Tris (pH 6.8), 8% (w/v) SDS, 40% (v/v) glycerol, 5% (v/v) β-mercaptoethanol, 0.04% (v/v) bromophenol blue). 10 μL sample per reaction was resolved on a 10 % or 15% acrylamide SDS-PAGE gel (180 V, 70 min). Gels were scanned using a ChemiDoc MP system with Cy3 and Cy5 multichannel settings (605/50 and 695/55, filters respectively) and stained with Coomassie after scanning. Experiments were done 3 times individually. Fluorescence was normalized to Coomassie staining and quantified with Image Lab (Bio-Rad). IC$_{50}$ curves were fitted with Graphpad Prism® 7 (Graphpad Software Inc.).

Western Blot. Western blots were performed as previously reported.[13] After the ABPP assay, the proteins on the SDS-PAGE gel were transferred to a membrane using a Trans-Blot Turbo™ Transfer system (Bio-Rad). For anti-FLAG antibody, Membranes were washed with TBS (50 mM Tris, 150 mM NaCl) and blocked with 5% milk in TBST (50 mM Tris, 150 mM NaCl, 0.05% Tween 20) for 1 h at RT. Membranes were then incubated with primary mouse anti-flag (0.02%) antibody in 5% milk TBST for 1 h at RT, washed with TBST, incubated with matching secondary antibody goat anti-mouse (0.02%) in 5% milk TBST for 1 h at RT and subsequently washed with TBST and TBS. The blot was developed in the dark using an imaging solution (10 mL luminol solution, 100 μL ECL enhancer and 3 μL 30% H$_2$O$_2$). Chemiluminescence was visualized using a ChemiDoc XRS (BioRad) with standard chemiluminescence settings.

Primary antibodies: monoclonal mouse-anti-FLAG (1:5000, Sigma Aldrich, F3156). Secondary antibodies: HRP-coupled-goat-anti-mouse (1:5000, Santa Cruz, sc2005).

5.5 References

1.   Cadas, H.; Gaillet, S.; Beltramo, M.; Venance, L.; Piomelli, D., Biosynthesis of an endogenous cannabinoid precursor in neurons and its control by calcium and cAMP. *J. Neurosci.* **1996,** *16* (12), 3934-3942.

2.   Cadas, H.; di Tomaso, E.; Piomelli, D., Occurrence and biosynthesis of endogenous cannabinoid precursor,N-arachidonoyl phosphatidylethanolamine, in rat brain. *J. Neurosci.* **1997,** *17* (4), 1226-1242.

3.   Ogura, Y.; Parsons, W. H.; Kamat, S. S.; Cravatt, B. F., A calcium-dependent acyltransferase that produces N-acyl phosphatidylethanolamines. *Nat. Chem. Biol.* **2016,** *12* (9), 669-71.

4.   Ohto, T.; Uozumi, N.; Hirabayashi, T.; Shimizu, T., Identification of novel cytosolic phospholipase A2s, murine cPLA2δ, ε, and ζ, Which form a gene cluster with cPLA2β. *J. Biol. Chem.* **2005,** *280* (26), 24576-24583.

5.   Lucas, K. K.; Dennis, E. A., Distinguishing phospholipase A2 types in biological samples by employing group-specific assays in the presence of inhibitors. *Prostag. Oth. Lipid M.* **2005,** *77* (1-4), 235-248.

6.   Dennis, E. A.; Cao, J.; Hsu, Y. H.; Magrioti, V.; Kokotos, G., Phospholipase A2 enzymes: physical structure, biological function, disease implication, chemical inhibition, and therapeutic intervention. *Chem. Rev.* **2011,** *111* (10), 6130-6185.

7.   Ghosh, M.; Tucker, D. E.; Burchett, S. A.; Leslie, C. C., Properties of the Group IV phospholipase A2 family. *Prog. Lipid Res.* **2006,** *45* (6), 487-510.

8.   Capestrano, M.; Mariggio, S.; Perinetti, G.; Egorova, A. V.; Iacobacci, S.; Santoro, M.; Di Pentima, A.; Iurisci, C.; Egorov, M. V.; Di Tullio, G.; Buccione, R.; Luini, A.; Polishchuk, R. S., Cytosolic phospholipase A(2)epsilon drives recycling through the clathrin-independent endocytic route. *J. Cell. Sci.* **2014,** *127* (P5), 977-993.

9.   Hussain, Z.; Uyama, T.; Kawai, K.; Binte Mustafiz, S. S.; Tsuboi, K.; Araki, N.; Ueda, N., Phosphatidylserine-stimulated production of N-acyl-phosphatidylethanolamines by Ca^{2+}-dependent N-acyltransferase. *BBA-Mol. Cell Biol. L.* **2018,** *1863* (5), 493-502.

10.   Binte Mustafiz, S. S.; Uyama, T.; Hussain, Z.; Kawai, K.; Tsuboi, K.; Araki, N.; Ueda, N., The role of intracellular anionic phospholipids in the production of N-acyl-phosphatidylethanolamines by cytosolic phospholipase A2ε. *J. Biol. Chem.* **2019,** *165* (4), 343-352.

11.   Baggelaar, M. P.; den Dulk, H.; Florea, B. I.; Fazio, D.; Bernabò, N.; Raspa, M.; Janssen, A. P. A.; Scavizzi, F.; Barboni, B.; Overkleeft, H. S.; Maccarrone, M.; van der Stelt, M., ABHD2 Inhibitor identified by activity-based protein profiling reduces acrosome reaction. *ACS Chem.l Biol.* **2019,** *14* (10), 2295-2304.

12. Baggelaar, M. P.; Janssen, F. J.; van Esbroeck, A. C. M.; den Dulk, H.; Allara, M.; Hoogendoorn, S.; McGuire, R.; Florea, B. I.; Meeuwenoord, N.; van den Elst, H.; van der Marel, G. A.; Brouwer, J.; Di Marzo, V.; Overkleeft, H. S.; van der Stelt, M., Development of an activity-based probe and in silico design reveal highly selective inhibitors for diacylglycerol lipase-alpha in brain. *Angew. Chem.-Int. Edit.* **2013,** *52* (46), 12081-12085.

13. van Esbroeck, A. C. M.; Janssen, A. P. A.; Cognetta, A. B.; Ogasawara, D.; Shpak, G.; van der Kroeg, M.; Kantae, V.; Baggelaar, M. P.; de Vrij, F. M. S.; Deng, H.; Allara, M.; Fezza, F.; Lin, Z.; van der Wel, T.; Soethoudt, M.; Mock, E. D.; den Dulk, H.; Baak, I. L.; Florea, B. I.; Hendriks, G.; de Petrocellis, L.; Overkleeft, H. S.; Hankemeier, T.; De Zeeuw, C. I.; Di Marzo, V.; Maccarrone, M.; Cravatt, B. F.; Kushner, S. A.; van der Stelt, M., Activity-based protein profiling reveals off-target proteins of the FAAH inhibitor BIA 10-2474. *Science* **2017,** *356* (6342), 1084-1087.
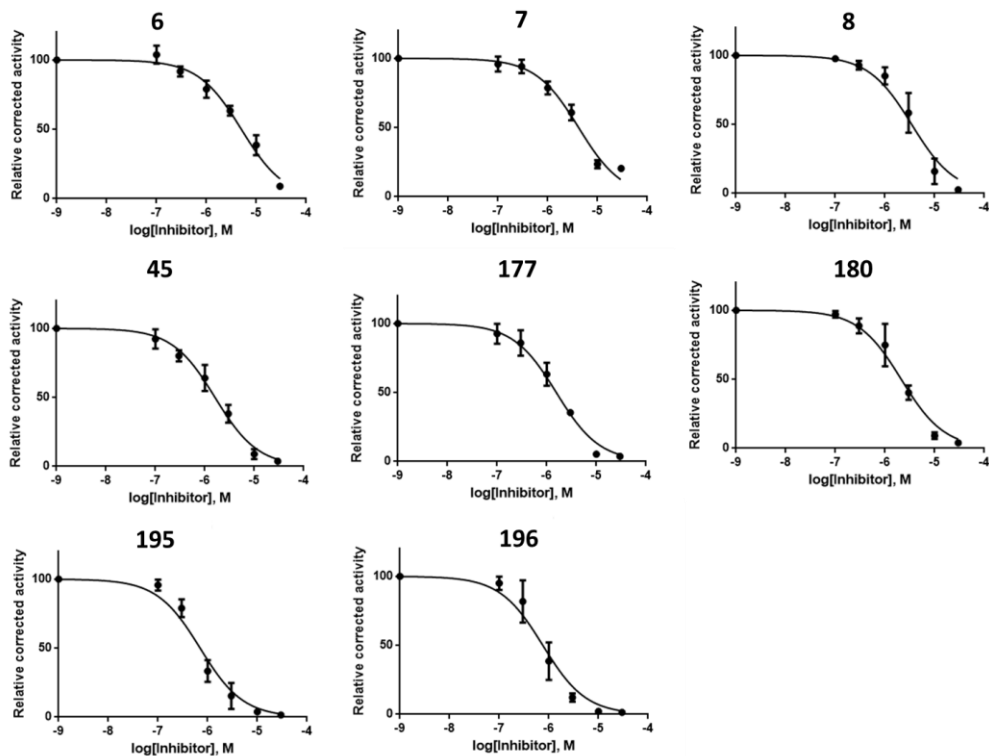
5.6 Supplementary Information

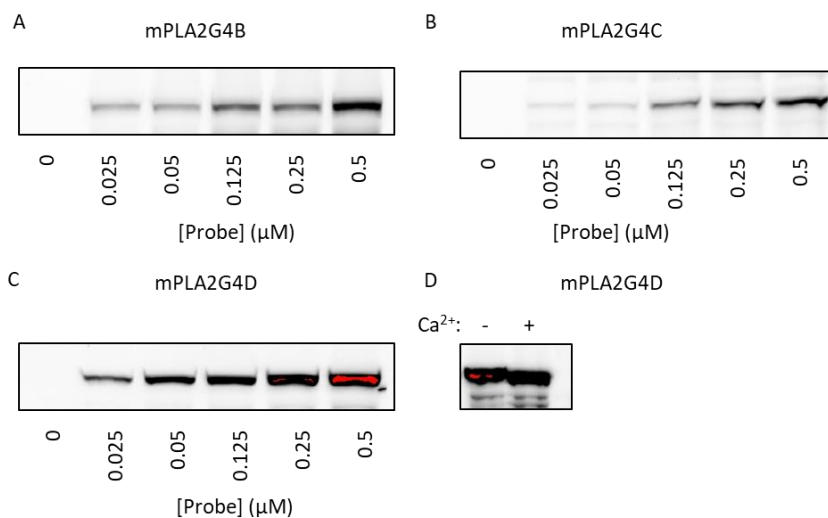**Figure S1**. Dose response curves of compounds which have been tested on hPLA2G4E (N=3).

Figure S2. Optimization of ABPP for mPLA2G4B, mPLA2G4C and mPLA2G4D. (A)&(B) Gel-based ABPP for optimization of the TAMRA-FP concentration (0; 0.025; 0.05; 0.125; 0.25; 0.5 µM, 20 min at RT) for the reaction with the cytosol fraction of mPLA2G4B and mPLA2G4C (1 µg/µL). (C) Gel-based ABPP for the TAMRA-FP concentration (0; 0.0125; 0.025; 0.05; 0.125; 0.25 µM, 20 min at RT) for the cytosol fraction of mPLA2G4D (0.5 µg/µL). (D) Gel-based ABPP for the difference of with and without calcium (3 mM) on mPLA2G4D (1.0 µg/µL) labelling by TAMRA-FP (0.5 µM, 20 min at RT). The samples are loaded on a 10% SDS-PAGE gel and Coomassie staining was used for the protein loading correction.
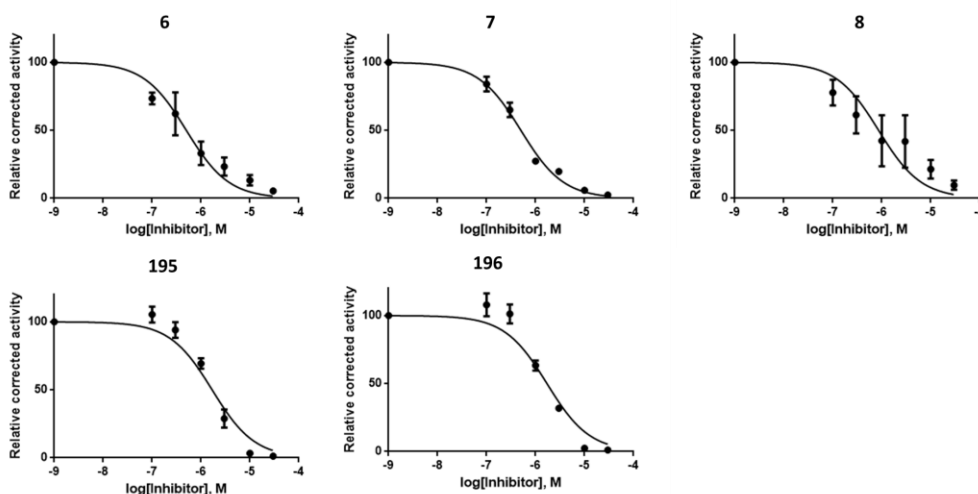

Figure S3. Dose response curves of compounds which have been tested on mPLA2G4D (N=3).

Table S1. Inhibitory activity of selected 8 compounds against mPLA2GB, mPLA2GC and mPLA2GD, respectively, in the gel-based ABPP assay. The data shows the residual protein activity in percentage and lower percentage number indicates high inhibitory activity of the inhibitor at 10 µM (N=1).

	6	7	8	45	177	180	195	196
mPLA2GB	100	98	90	63	62	60	58	71
mPLA2GC	100	89	82	100	100	100	100	98
mPLA2GD	14	6	12	58	41	28	8	4